This is a peer-reviewed, accepted author manuscript of the following research article: Chen, M, Lu, J, Felfel, RM, Parsons, AJ, Irvine, DJ, Rudd, CD & Ahmed, I 2017, 'Wet and dry flexural high cycle fatigue behaviour of fully bioresorbable glass fibre composites: in-situ polymerisation versus laminate stacking', Composites Science and Technology, vol. 150, pp. 1-15. https://doi.org/10.1016/j.compscitech.2017.07.006

Wet and Dry Flexural High Cycle Fatigue Behaviour of Fully Bioresorbable Glass Fibre Composites: In-situ Polymerisation versus Laminate Stacking

Menghao Chen[a], Jiawa Lu[b*], Reda M. Felfel[a, e], Andrew J. Parsons[c], Derek J. Irvine[d], Christopher D. Rudd[b], Ifty Ahmed[a*]

[a] Advanced Material Research Group, Faculty of Engineering, University of Nottingham, University Park, Nottingham, UK, NG7 2RD

[b] Department of Mechanical, Materials and Manufacturing Engineering, University of Nottingham Ningbo China, 199 Taikang East Road, Ningbo, 315100, China

[c] Composites Research Group, Faculty of Engineering, University of Nottingham, University Park, Nottingham, UK, NG7 2RD

[d] Department of Chemical and Environmental Engineering, Faculty of Engineering, University of Nottingham, University Park, Nottingham, UK, NG7 2RD

[e] Physics Department, Faculty of Science, Mansoura University, 35516, Egypt

Abstract

Fully bioresorbable phosphate based glass fibre reinforced polycaprolactone (PCL/PGF) composites are potentially excellent candidates to address current issues experienced with use of metal implants for hard tissue repair, such as stress shielding effects. It is therefore essential to investigate these materials under representative loading cases and to understand their fatigue behaviour (wet and dry) in order to predict their lifetime in service and their likely mechanisms of failure. This paper investigated the dry and wet flexural fatigue behaviour of PCL/PGF composites with 35% and 50% fibre volume fraction (V_f). Significantly longer flexural fatigue life ($p<0.0001$) and superior fatigue damage resistance were observed for In-situ Polymerised (ISP) composites as compared to the Laminate Stacking (LS) composites in both dry and wet conditions, indicating that the ISP promoted considerably stronger interfacial bonding than the LS. Immersion in fluid (wet) during the flexural fatigue tests resulted in significant reduction ($p<0.0001$) in the composites fatigue life, earlier onset of fatigue damage and faster damage propagation. Regardless of testing conditions, increasing fibre content led to shorter fatigue life for the PCL/PGF composites. Meanwhile, immersion in degradation media caused softening of both LS and ISP composites during the fatigue tests, which led to a more ductile failure mode. Among all the composites that were investigated, ISP35 (35% V_f) composites maintained at least 50% of their initial stiffness at the end of fatigue tests in both conditions, which is comparable to the flexural properties of human cortical bones. Consequently, ISP composites with 35% V_f maintained at least 50% of its flexural properties after the fatigue failure, which the mechanical retentions were well matched with the properties of human cortical bones.

Keywords: A. Glass fibre, B. Fatigue, C. Damage mechanics, D. Life prediction, In-situ polymerisation

**Corresponding author at:* Advanced Material Research Group, Faculty of Engineering, University park,

University of Nottingham, UK, NG7 2RD.

Laminate Stacking (LS)

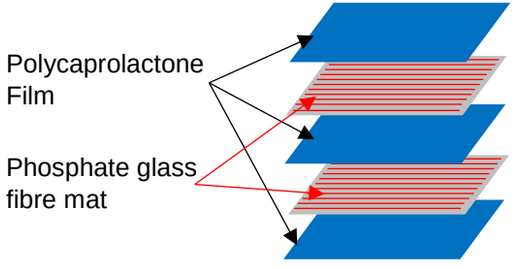

Hot Compression Moulding

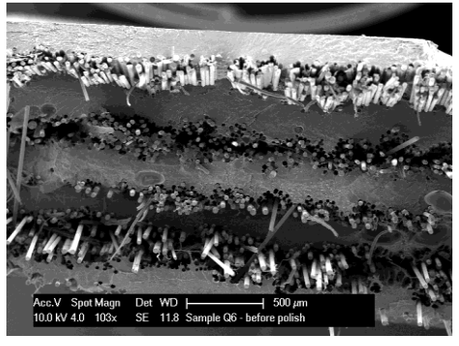

In-situ Polymerization (ISP)

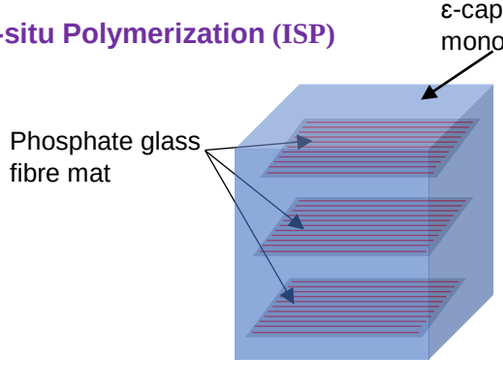

Polymerization

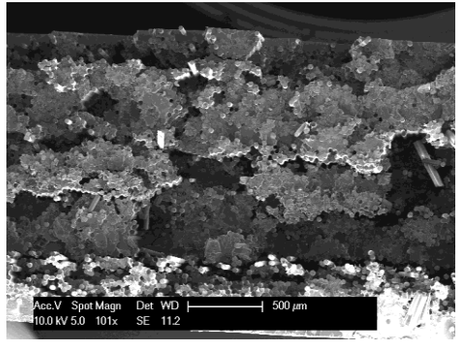

Flexural Fatigue

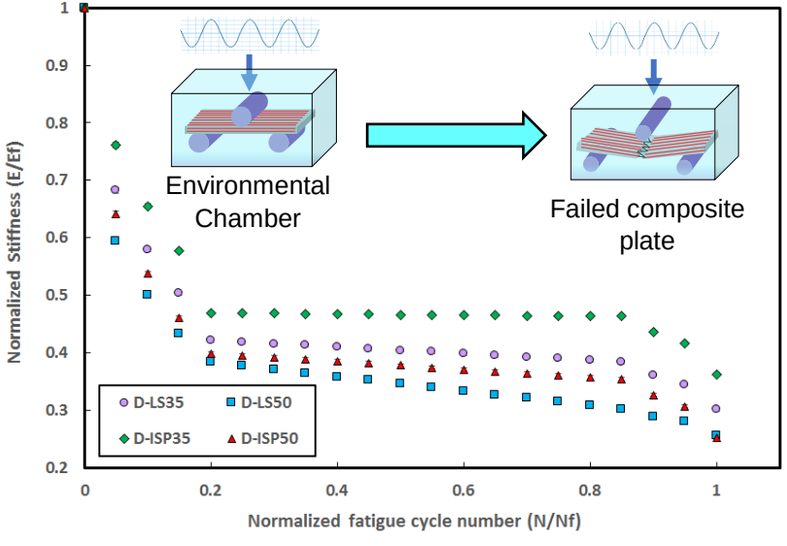

Tel: +44 (0)1157484675; +86(0)57488180000 (ext. 8238).
Email address: Ifty.ahmed@nottingham.ac.uk; jiawa.lu@nottingham.edu.cn.

1. Introduction

In recent decades, fully bioresorbable polymer composites with appropriate biocompatibility and mechanical properties has provided an exciting opportunity to replace conventional metal alloy implants, and it has become an active research field because of its excellent potential in the field of hard tissue repair [1, 2]. Bioresorbable fibre reinforced composites have been extensively studied utilising different glass fibre compositions, polymer matrices, fibre architectures and volume fractions. Their mechanical properties range between 200-700 MPa flexural strength and 15-25 GPa flexural modulus [3-9].

Polycaprolactone (PCL)/Phosphate based glass fibre (PGF) composites have been investigated for developing fully bioresorbable implants [10-13]. PGFs have the ability to fully dissolve within aqueous media and with adjustable degradation rate [10]. Both PGF and PCL have also been proven to have good biocompatibility and are considered favourable materials for biomedical application [3, 4, 14]. However, achieving satisfactory fibre-matrix interface adhesion and retention, thus appropriate composite mechanical properties for bone fracture fixation has been the main restriction [3, 5, 6, 15]. Studies have recognised the weak fibre-matrix interface is mainly due to poor fibre impregnation, which can result from the high viscosity of the melted matrix involved in traditional laminate stacking (LS) and hot press moulding [5, 13, 16]. To promote a more durable fibre-matrix interface, a novel in-situ polymerisation (ISP) technique has been developed to manufacture PCL/PGF composites in the group [16, 17]. There is solid evidence that suggested that ISP can promote a significantly stronger and more robust fibre-matrix interface than LS, with accordingly higher mechanical properties and prolonged retention of properties during degradation [13, 16-19]. Furthermore, the biocompatibility of the ISP PCL was investigated via Alamar blue assay using osteoblasts derived from human craniofacial bone cells. The results indicated that ISP PCL was highly biocompatible, and the residual monomer (Measured by Nuclear Magnetic Resonance) did not significantly affect the biocompatibility of the composites [19].

The flexural fatigue properties are of vital importance for bone fracture fixation implant applications. The main application for the PCL/PGF composites is as bone fracture fixation devices and has initially focused on bone repair plates, for which the primary loading would

be in flexure mode and as such was the focus for this study [20-22]. Typical time required for bone fracture healing is 8-12 weeks, where the composites will be subject to dynamic body fluid and constant body temperature [20, 21, 23]. The majority of previous studies on fibre reinforced composites have indicated that elevated humidity and temperature generally severely shortened their fatigue life [24-27]. Composites fatigue behaviour is a complex phenomenon, which is generally studied by crack initiation, crack multiplication and final failure [28-30]. Damage mechanisms in flexural fatigue of fibre reinforced composites, in general, involve matrix cracking, fibre breakage and interface failure [31, 32]. The diffusion and growth of composites fatigue damage resulting from crack bridging and/or fibre/matrix de-bonding is governed by the behaviour of fibre/matrix interaction [31, 33-35]. The diffuse damage growth often results in a gradual decrease of the composite's stiffness with growing loading cycles, which is coupled with a significant increase in the composite's material damping [36]. The damping mechanisms of fibre reinforced composites are governed mainly by thermo-elastic damping, Coulomb friction damping of the fibre-matrix interface, energy dissipation at cracking/delamination and the viscoelastic nature of the fibre and matrix material [37, 38]. Both stiffness evolution and material damping are often used as sensitive indicators to study the damage mechanisms of composites [39-43]. Shah [44] systematically studied the stiffness evolution of plant fibre reinforced composites subjected to tensile fatigue loading, where stiffness profiles were used to investigate composite damage initiation and accumulation. Gassan [38] investigated the fatigue behaviour of natural fibre (flax and jute) reinforced polymer composites using specific damping capacity (SDC) as a sensitive indicator for monitoring the behaviour of material damage.

Despite the extensive studies on the mechanical performance of implant biomaterials, their time-dependent fatigue behaviour is still poorly understood. Fatigue properties are of paramount importance for their intended application where components are subjected to various loading and environmental parameters, which vary with time over the period of service. The target properties of the composites were within the properties reported for human cortical bone, i.e. 5-23 GPa and 35-280 MPa for flexural modulus and strength respectively [45]. There are several studies of fatigue behaviour for metal alloy and bone cement composite implant biomaterials, which well pointed out the significance of fatigue strength and life in the design and use of implant devices [46]. However, up to the best of

the authors knowledge, cyclic fatigue response of the fully resorbable composites has not been explored yet.

In this study, PCL/PGF composites with V_f of 35% and 50% were produced using LS and ISP techniques. Environmental flexural fatigue tests were performed on these composites in both dry conditions at ambient temperature and in wet conditions immersed in phosphate buffered saline (PBS) solution at 37 °C. The wet conditions were intended to mimic the physiological nature of the human body. Both stiffness reduction and SDC were used as sensitive indicators to monitor the damage initiation of the composites during cyclic loading. The influences of solution immersion, fibre content and fibre-matrix adhesion on the performance of the PCL/PGF composites were investigated by comparing their fatigue behaviour.

2. Materials and Methods

2.1. Materials

Monomer ε-caprolactone (97% purity), $Sn(Oct)_2$ (92.5%-100% purity) and benzyl alcohol (99.8% purity) were obtained from Sigma Aldrich (UK). PCL pallets were also obtained from Sigma Aldrich (UK) and with a molecular weight (M_w) of ~65,000 g/mol.

2.2. Phosphate based glass and glass fibre

Phosphate based salts were used to produce fully bioresorbable phosphate glass (Sigma Aldrich, see Table 1 for detailed glass formulation). A specific salt mixing and melting scheme was used to produce the phosphate based glass. PGFs were made using in-house designed melt-draw equipment comprised of a furnace (Lenton Furnaces, UK) with a Pt/10% Rh crucible (Johnson Matthey, UK). Phosphate glass and glass fibre mats were stored in a desiccator to minimise any potential moisture adsorption. The fibre mats were then dried in a 50 °C vacuum oven for 24 hours before use. For the detailed manufacturing process and parameters, please refer to the authors' previous paper [13].

2.3. PCL/PGF composites

Composites with 35% and 50% fibre volume fraction (V_f) were manufactured via both ISP and LS. Respective composite codes and specifications are listed in Table 2.

2.3.1. Laminate stacking (LS) technique

PCL thin films were manufactured and PGF mats were stacked with the thin films to hot compress into composites. Detailed processes can be found in the authors' previous paper

[13]. The composite plate was made into test specimens with dimensions of 40mm × 15mm × 2mm by a band saw.

2.3.2. In-situ polymerisation (ISP) technique

PTFE moulds with two injection ports were designed and used to produce PCL/PGF composites in one single step. ε-caprolactone was degassed via a freeze-thaw-pump process to minimise the moisture content within the solution. Reaction mixture of ε-caprolactone with pre-determined amount of catalyst and initiator was injected into the mould cavity and PCL was polymerised directly around the PGF mats. Ring opening polymerisation was utilised for PCL polymerisation during the ISP process. Detailed mould design and explanation of the in-situ process can be found in author's previous paper [13]. Resulting composite plates were cut into dimensions of 40mm × 15mm × 2mm using a band saw.

2.4. Flexural testing

2.4.1. Monotonic loading

Monotonic 3-point bending tests were conducted on a Bose ElectroForce® Series II 3330 testing machine. The testing machine is equipped with an environmental chamber, which enables tests within liquid at various temperatures (See Figure 1). BS EN ISO 14125:1998 was followed for all tests. Sample dimensions of 40mm × 15mm × 2mm, a cross-head speed of 1 mm/min and a 3 kN load cell was used. Tests were carried out in triplicate (n=3). Composites were tested in two environments: at ambient temperature and in dry conditions (Dry Environment) and at 37 °C submerged in PBS solution (Wet Environment). The samples were immersed in PBS heated to 37°C for 5 minutes to allow PBS and testing temperature equilibrate prior to testing. Displacement/deflection loads were measured via the testing machine, for which the stress and strain were calculated according to the equations stated in BS EN ISO 14125:1998 as below:

$$\sigma_f = \frac{3FL}{2bh^2} \qquad (1)$$

$$\varepsilon = \frac{6sh}{L^2} \qquad (2)$$

Where ε is the strain, σ_f is the stress, s is the measured displacement, F is the measured load, b is the sample width, h is the sample thickness and L is the sample span length.

2.4.2. Cyclic loading

Flexural fatigue tests (Load-controlled) were conducted on a Bose ElectroForce® Series II 3330 testing machine. Figure 2 presents a sample load waveform (5 Hz) applied during the fatigue tests (Specific fatigue terms and R-values defined). In accordance with BS ISO 13003:2003, at least 5 samples were examined to failure at six stress levels for the determination of the composites' stress-lifetime diagrams. All the composites were tested in 3-point bending mode (Bending-bending condition) with a stress ratio of R = 0.1. Calculations for flexural stress and strain were performed according to BS EN ISO 14125:1998. Shear effects were taken into consideration for the stress and strain calculations since the defection of the specimens during the fatigue tests was relatively large.

When the measured deflection was less than 10% of the sample span length, the flexural stress and strain were calculated via equation 1 and 2. When the measured deflection was larger than 10% of the sample span length, equation 3 and 4 below were used:

$$\sigma_f = \frac{3FL}{2bh^2}\left\{1 + 6\left(\frac{s}{L}\right)^2 - 3\left(\frac{sh}{L^2}\right)\right\} \qquad (3)$$

$$\varepsilon = \frac{h}{L}\left\{6\frac{s}{L} - 24.37\left(\frac{s}{L}\right)^3 + 62.17\left(\frac{s}{L}\right)^5\right\} \qquad (4)$$

Where σ_f is the flexural stress, ε is the strain, s is the beam mid-point deflection, F is the load, L is the span length, h is the thickness of the specimen and b is the width of the specimen.

Fatigue tests were performed in both dry and wet testing conditions. Testing the dry composites at room temperature was known as the dry testing condition and wet testing condition referred to testing the submersed composites in PBS solution and at 37 °C. A KTJ TA318 thermometer & hygrometer was used to measure the temperature and relative humidity of the dry testing conditions, which were in the range of 15 °C - 22 °C and 44% - 53% respectively. Stress levels for all fatigue tests were 80%, 70%, 60%, 50%, 40% and 30% of the corresponding Ultimate Flexural Strength (UFS) for each type of composite.

Figure 3 showed an example of the stress strain variation of a composite sample during fatigue testing. The loading cycles plotted were selected as 1 out of every 1000 loading cycles and each loop in Figure 3 represents a full loading cycle. Flexural stiffness of the

composite can be calculated from each loading cycle and the variation in their strain can also be recorded.

2.5. Fatigue data analysis

2.5.1. Stress-Life (S-N) diagram

As illustrated in Figure 4, a typical Wohler Stress-Life (S-N) diagram [31] is plotted as stress amplitude (σ_a) against number of fatigue cycles to failure (N_f) (See Figure 4). S-N curves are normally fitted with a power regression relationship, named Basquin's equation (Equation 5) [31].

$$\sigma = aN_f{}^b \quad (5)$$

Where σ is a generic term describing cyclic stress (in this case σ_a, see Figure 2), N_f is a generic term describing fatigue life (in this case cycles to failure) and *a* & *b* are material constants specific to each material. The constant '*b'* is used as an important parameter in this study to indicate the sensitivity of the fatigue life to the applied stress. The value of '*b'* represents the slope of the SN curve, thus the decline rate of fatigue strength.

2.5.2. Specific Damping Capacity (SDC)

To study and monitor the progress of composite damage during the fatigue tests, SDC was used as a sensitive indicator throughout this study. As damage progresses, the composite specimens show reductions in strength and modulus as well as a significant increase in their own damping [38, 47]. Changes in material damping capacity can be observed as a function of the stress levels during the fatigue tests [48]. An example is illustrated graphically in Figure 5.

In this paper, SDC was measured to determine the critical applied stress (CAS) for damage initiation of both the LS and ISP composites within 104 fatigue loading cycles. This cycle number (104) was chosen since it is the general divider between low and high cycle fatigue behaviour [31]. A similar method was used by Gassan et. al to measure the CAS values for studying fatigue damage behaviour of fibre reinforced composites [38]. The CAS is an important factor for load bearing applications, such as fracture fixation devices, as it sets the limitations of the composite loading capacity under cyclic loading conditions. Any applied cyclic stress higher than the measured CAS would imply material damage within 104 loading cycles.

In order to obtain SDC values for the composites, a fatigue test is performed using constant values of stress level, R and frequency (R=0.1, 5 Hz) for a defined number of load cycles (10^4 cycles in this case). Fresh LS and ISP composites (non-degraded) were used for the SDC study. Subsequently, the fatigue test was repeated for the same number of load cycles at a higher stress levels. This continued until the specimen failed. A minimum of n=5 samples were tested for each category of composites. Tests were carried out in both dry and wet testing conditions, using the stress levels specified in 2.4.2. The value of SDC was then calculated using Equation 6 [38, 49]:

$$SFDC = \Delta U/U = (U_I - U)/U \qquad (6)$$

Where U is the maximum strain energy stored by the specimen during one loading cycle, ΔU is the energy dissipated only by the specimen during one loading cycle (such as friction damping caused by de-bonding, crack and delamination) and U_I is the input energy from the system to the specimen during one cycle. Strain energy was calculated by integrating the area within the loading loop (See Figure 3 shaded area) at a defined number of load cycles. Input energy was calculated by integrating the loading and displacement history from the testing machine.

2.6. Scanning Electron Microscopy (SEM)

SEM was performed on freeze-fractured specimens after testing to study the matrix/fibre interface and failure mode. 10 keV Voltage was applied with secondary electron mode. Platinum was sputter-coated on all composites samples before imaging.

2.7. Burn off test

Actual fibre volume fractions of both LS and ISP composites were determined by burn off tests. BS EN ISO 2782-10 was applied for all burn off tests. Table 3 reports all results (n=5).

2.8. Statistical analysis

Data were presented in tables and figures as mean ± standard deviation. Microsoft Excel was used to analyse the data and a student's unpaired t-test was performed to determine the statistical significance as below: statistically insignificant ($p>0.05$), statistically significant ($p<0.05$), very statistically significant ($p<0.01$) and extremely statistically significant ($p<0.0001$).

3. Results

3.1. Composites fibre content and quasi-static flexural properties

Table 3 below shows the fibre volume fractions, quasi-static flexural strength and modulus for all the LS and ISP composites tested in both dry and wet testing conditions.

3.2. S-N diagrams

Figure 6 shows the variation of the fatigue life for each of the composites tested versus increasing stress levels in both dry and wet testing conditions. A good fit can be seen from the Basquin's equation (Equation 5) to the experimental data, with R^2-value > 0.9 for all regressions. Table 4 shows the values of *'b'* obtained from curve fitting the experimental fatigue data using the Basquin's equation.

A gradual decrease in fatigue life with increasing stress levels was observed for all composites, as expected. It was also observed that the 35% V_f composites showed a significantly longer fatigue life ($p<0.01$) than their equivalent 50% V_f composites (See Figures 6a and 6b). In dry conditions at the same stress level, D-LS35 and D-ISP35 showed ~29% and ~34% longer fatigue life respectively, when compared to D-LS50 and D-ISP50. However, in wet conditions, the W-LS35 and W-ISP35 showed ~20% and ~23% longer fatigue life than W-LS50 and W-ISP50.

Comparing Figures 6a and 6b, immersion in PBS solution at 37 °C substantially decreased the fatigue life for both ISP and LS composites. At the same stress level, the dry D-LS35 and D-LS50 samples showed approximately 10 times longer fatigue life than the wet W-LS35 and W-LS50 samples respectively. For example, D-LS35 exhibited ~3 million cycles to failure at 30% UFS stress level, whilst the wet W-LS35samples lasted only ~50,000 cycles. Similarly, D-ISP35 and D-ISP50 exhibited approximately 9 times longer fatigue life than W-ISP35 and W-ISP50 (i.e. ~4 million and ~230,000 cycles to failure for D-ISP35 and W-ISP35 respectively at 30% UFS stress level).

Regardless of the testing conditions, the ISP composites demonstrated a substantially longer fatigue life ($p<0.0001$) than the LS composites of equivalent V_f. When tested in a dry environment and at the same stress level, the D-ISP35 and D-ISP50 showed ~25% and ~19% longer fatigue life than D-LS35 and D-LS50 respectively (See Figure 6a). Similarly, in wet conditions, the W-ISP35 and W-ISP50 exhibited ~85% and ~74% longer fatigue life than W-LS35 and W-LS50 (See Figure 6b).

3.3. Failure strain variation

Figures 7a and 7b show the variation of failure strain versus the stress levels tested. The vertical dotted line represents the threshold stress level at which the failure strains increase significantly ($p<0.01$). The LS composites showed significantly lower failure strain profiles ($p<0.01$) than ISP composites in both dry and wet conditions. By comparing ISP and LS composites (identical V_f) in dry conditions (See Figure 7a), no significant difference ($p>0.01$) was found in the increase rate of failure strain with increasing stress levels. However, in wet conditions, the W-ISP50 samples showed a significantly faster increase rates of failure strain than the W-LS50 (See Figure 7b).

When tested in the same conditions, both LS and ISP composites with 50% V_f showed significantly lower ($p<0.01$) failure strain values in comparison to composites with 35% V_f for all stress levels. Figures 7a and 7b, also showed that the LS and ISP composites had significantly higher failure strain value profiles ($p<0.01$) in dry conditions compared to wet conditions. When tested dry, the failure strain value of D-LS35 and D-LS50 started to increase at 50% UFS stress level, while 60% UFS stress level (See the dotted vertical line in Figure 7) was observed for D-ISP35 and D-ISP50. However, in wet conditions, the increase was observed from 40% UFS stress level for all LS and ISP composites.

3.4. Stiffness evolution

The stiffness evolution profiles are presented in Figures 8a and 8b below, which show gradual decline of the composites' stiffness during their fatigue life at a specific stress level (40% of UFS). The initial stiffness E_f was determined from the first loading cycle and the residual stiffness, *E* at *n* cycles of the loading loop (See Figure 3).

Substantial differences were observed when comparing the stiffness at failure, following the trend of D-ISP35 > D-LS35 > D-ISP50 > D-LS50 > W-ISP35 > W-LS35 > W-ISP50 > W-LS50 for all stress levels investigated. For example, at 40% UFS stress level, D-ISP35 exhibited ~60% stiffness at failure whilst W-LS50 demonstrated ~30% residual stiffness at failure.

Comparing Figures 8a and 8b, the ISP composites revealed significantly higher stiffness profiles ($p<0.01$) than the LS composites through their entire fatigue life. Moreover, composites with 35% V_f showed considerably higher stiffness profiles throughout the fatigue life and slower stiffness reduction rates than composites with 50% V_f in the same testing condition. The change from dry to wet condition resulted in significantly lower

stiffness profiles ($p<0.01$) and faster stiffness reduction rates ($p<0.01$) for all the LS and ISP composites.

According to Figure 8a, there was a distinct increase in stiffness at the beginning of the composites fatigue life in dry conditions. Meanwhile, in wet conditions, the stiffness profiles showed a gradual decline from the beginning of the fatigue life (See Figure 8b). Moreover, in dry testing conditions, it was found that with tests performed at stress levels over 50% of respective UFS, no initial increase was seen and a gradual decline from the beginning of the fatigue tests was also observed (See inset graph of Figure 8a).

3.5. Specific Damping Capacity (SDC)

Figure 9 shows the variation of SDC versus increasing maximum applied stress for both LS and ISP composites tested in dry and wet conditions. The critical applied stress (CAS) for damage initiation of the composites was estimated as the stress where SDC starts to increase significantly ($p<0.01$) and they are indicated by arrows in Figure 9 [38].

Table 5 showed the CAS values for all composites tested. Regardless of the testing environment, significantly higher CAS ($p<0.01$) values can be seen for ISP composites than for the LS composites. Moreover, with the same manufacturing method and in dry conditions, composites with 35% V_f showed significant higher CAS ($p<0.01$) than composites with 50% V_f. Meanwhile, 50% composites showed lower CAS values than 35% composites in wet conditions. In dry conditions (Figure 9a), only D-LS50 had significantly higher SDC profile ($p<0.01$) against increasing applied stress than other composites. However, in wet conditions (Figure 9b), both W-LS35 and W-LS50 showed distinctly higher SDC profiles ($p<0.01$) than W-ISP35 and W-ISP50 respectively. By comparing Figures 9a and 9b, the CAS values for W-LS35, W-LS50, W-ISP35 and W-ISP50 were ~30%, ~41%, ~41% and ~49% lower than D-LS35, D-LS50, D-ISP35 and D-ISP50 respectively.

3.6. SEM Analysis

Figure 10 compared the cross sections of the composite fracture surfaces between LS and ISP composites tested within both dry and wet conditions. Clear polymer rich zones and fibre pull-outs were seen from the SEM micrographs of LS35 and LS50 (Figure 10a, 10e and Figure 10c, 10g). Meanwhile, clean fibre fractures with no visible polymer rich zones were observed from the SEM micrographs of ISP35 and ISP50 (Figure 10b, 10f and Figure 10d, 10h).

Figure 11 displayed the typical fatigue failure modes of the LS and ISP composites tests in both dry and wet conditions. In dry conditions, LS composites showed compressive delamination and interlaminar shear fracture failure modes (Figure 11a and 10b), whilst ISP composites showed clean centre fracture (Figure 11c). In wet conditions, the LS composites showed softening behaviour with interlaminar shear fracture failure mode (Figure 11d and 11e), whilst the ISP composites showed fibre sliding behaviour with centre fracture failure mode (Figure 11f).

4. Discussions

This study investigated the cyclic flexural fatigue performance of PCL/PGF composites (V_f of 35% and 50%) produced via LS and ISP processes. Environmental conditions were evaluated by performing tests in dry (room temperature) and in wet conditions (immersed in PBS at 37 °C). Fatigue behaviour of the composites was characterised via the classic S-N diagrams, stiffness degradation profiles and specific damping capacity (SDC).

Table 3 summarises the quasi-static flexural properties of the LS and ISP composites in both dry and wet conditions. Testing the samples in wet conditions revealed significant reductions in both the stiffness and strength of the composites, compared to the dry tested samples. Several studies have been conducted on similar PGF composites, which investigated quasi-static mechanical properties in dry and wet conditions. They also reported a distinct decrease in flexural strength and modulus for samples tested in quasi-static wet conditions, and suggested this was due to media attack disrupting the fibre matrix interface and plasticisation [3, 5, 13, 50]. However, the ISP composites revealed considerably higher flexural properties compared to the LS composites in both dry and wet conditions. A previous study [13] revealed that a stronger and more robust fibre/matrix interface was promoted by the ISP process as compared to LS, which inhibited PBS media attack and revealed a significant increase in the composite flexural properties (by ~45%).

Factors influencing the fatigue behaviour were characterised taking into consideration three key factors as discussed below.

4.1. Influence of fibre-matrix interface

The S-N diagrams produced revealed the fatigue life profiles with increasing testing stress for all the LS and ISP composites tested (See Figure 6). It was immediately apparent that the ISP composites demonstrated a significantly longer fatigue life ($p<0.0001$) than the LS composites at each stress level in both dry and wet conditions. This major increase in

fatigue life was attributed to sturdier interfacial bonding achieved by the ISP manufacturing process. De-bonding of the fibre/matrix interface (especially ductile matrices, such as PCL) is widely considered to be the main governing factor of crack propagation, which can lead to fatigue failure of fibre reinforced composites [31, 51, 52]. Weak interfacial properties can allow de-bonding and friction sliding between fibre and matrix to occur readily upon crack propagation, which can lead to matrix cracks (In this case delamination, see Figures 11a and 11b) without major fibre fractures [33, 53]. Conversely, a stronger fibre/matrix interface could inhibit interfacial sliding and lead to direct fibre fractures along with cracks in the matrix, without inducing significant de-bonding of the fibre/matrix interface (see Figure 11c) [33, 51, 53]. This difference in behaviour was apparent when comparing ISP and LS composites, as illustrated by the failure cross sections in Figure 10. LS composites showed significant fibre pull-out and ISP composites had clear fibre fractures, which demonstrated that a stronger fibre/matrix interface for the ISP samples had been achieved. Several studies have investigated the effects of the fibre/matrix interface on the fatigue behaviour of glass or carbon fibre reinforced composites. The studies applied coupling agents on fibre surfaces to promote stronger interfacial bonding with the polymer matrices and consequently significantly longer fatigue lives (ranging from 5% - 20%) were achieved [38, 47, 52, 54]. It should be noted that improvements in fibre/matrix interfacial properties in this study were achieved via the ISP manufacturing process alone, and without the use of coupling or sizing agents. This suggests that the ISP process can promote strong interfacial bonding of fibre reinforced composites and has huge potential to further improve the mechanical properties with use of appropriate coupling agents [16].

The variation in specific damping capacity (SDC) was applied in this study to monitor the anisotropic composites' critical applied stress (CAS) for damage initiation during fatigue loading. Figures 9a and 9b both indicated that the ISP composites retained distinctly higher ($p<0.01$) normalised critical load for damage initiation than the LS composites at equivalent V_f, indicating that the fatigue damage initiation of the composites was postponed by the ISP technique. This suggested that the improvement of interfacial strength led to higher critical applied loads (60% - 70% under dry conditions and 20%-30% under wet conditions) for the on-set of progressive composite fatigue damage. Similar behaviour was also reported by Gassan et al. [38] on investigations of tension-tension fatigue of natural fibre reinforced composites (made by resin transfer moulding), where 10%-30% increase in values of Critical Applied Load (CAL) for damage initiation were achieved via application of alkaline

and saline coupling agents. Flexural fatigue studies conducted on unidirectional (UD) glass fibre reinforced epoxy composites, revealed that a stronger fibre-matrix interface via treatment using a commercial saline coupling agent delayed the matrix cracking, thus increasing the fatigue life of the UD composites by ~20% [55, 56].

It was also observed that the LS composites had significantly lower failure strain ($p<0.05$) than the ISP composites (Equivalent V_f), which exhibited that the ISP composites could sustain increased plastic deformation and damage than their LS counterparts before fatigue failure (See Figure 7). Similar findings were reported for unidirectional glass fibre composites, for which failure strain increased with improved fibre/matrix interfacial properties by applying saline coupling agents [55]. From Figures 7a and 7b, a sudden increase in the failure strain was observed for both LS and ISP composites, where the critical stress levels for the onset of the failure strain increase were found to be identical to the critical loading levels in SDC (60% and 50% of UFS for D-ISP35/50 and D-LS35/50 respectively, 40% for all composites in wet conditions). This relationship between SDC and failure strain for the PCL/PGF composites provided strong evidence that the critical stresses for onset of significant fatigue damage observed in this study correlated well and should be taken into consideration.

4.2. Influence of fluid immersion

It was also observed that the wet testing conditions led to a significant decrease ($p<0.0001$) in the fatigue life of the PCL/PGF composites, with a 10 and 9-fold reduction observed in LS and ISP composites respectively (See Figure 6). Deterioration of the fatigue strength in wet conditions was also noted as the slopes of the SN diagram became significantly steeper from dry to wet conditions (represented by coefficient ‘b’, in Table 4). Fluids, such as water and PBS solution, are able to diffuse into the composites and weaken both the matrix and the fibre/matrix interface [57]. Our previous study [13] showed that the fibre/matrix interface plasticisation for both ISP and LS composites occurred readily at 37 °C in PBS. Degradation of PGFs at or near the PGF fibre/matrix interface within PBS solution can further influence the fibre/matrix bonding leading to reduction of composite mechanical properties. Degradation of the fibre/matrix interface is known to increase the damage accumulation rate under cyclic fatigue loading, hence significantly reducing fatigue life [57, 58]. Similar reductions in fatigue life were also reported by several studies on glass and carbon fibre reinforced composites and degradation of fibre/matrix interface was stated as the main cause [57, 59-61]. Liao et al. [59] investigated flexural fatigue on vinyl ester/E-

glass composites in water and NaCl solutions at ambient temperature. They observed significant reductions in fatigue life at low stresses in both media. McBagonluri et al. [60] also investigated UD pultruded E-glass/vinyl ester composites subjected to flexural environmental fatigue tests performed in a fluid cell with salt water at 65 °C. They reported that fatigue life was considerably reduced (~55%) due to fluid immersion. Furthermore, a flexural fatigue study conducted by Sumsion et al. [62] on UD graphite/epoxy composites in water and air at ambient temperature, revealed a significant decrease in fatigue life (~47%) which was suggested to be caused by water attack of the fibre/matrix interface.

It was further observed that at high testing stress levels (70% & 80% of UFS), there were no vast differences in the composites' fatigue life between dry and wet testing conditions (See Figure 6). A significant difference only began to emerge when the composites were tested at lower stress levels (30%~60% of UFS). This behaviour suggested that damage accumulation progressed slower at lower stress levels for LS and ISP composites. Meanwhile, higher stress levels resulted in stress-dependent fatigue behaviour resulting in faster damage accumulation. This behaviour was also reported by Liao et al. [59] investigating fatigue behaviour of E-glass/vinyl ester composites, which showed that the composites fatigue life was stress-dominated at higher stress levels.

It was evident from Figure 8a that, in the dry environment, an initial increase in stiffness at the early stage of the composites' fatigue life (~5% of N_f) had occurred, before the gradual decline to failure. One possible explanation was due to the presence of voids and void tunnels inside the composites, which had perhaps closed due to the applied cyclic loading, making the composites more compact and stiffer. This explanation was supported by the fact that the LS composites showed a larger increase in stiffness than the ISP composites (See Figure 8a), and it was previously reported that LS composites generally possessed higher void content than their ISP counterparts [13]. However, it is very difficult to observe or measure this behaviour during the fatigue tests, which distinctive proves of the voids collapsing were not found.

Another possible explanation for this observation could be due to reorientation of any initially off-axis fibre filaments. During the fibre manufacture, the initial fibres collected on the fibre winding drum were sprayed with PCL solution (Mixed with Chloroform) to maintain alignment. However, the removal of PCL coated fibre from the drum and the insertion into the composite manufacturing moulds could have caused some fibres to become miss-

aligned. Furthermore, since the phosphate glass fibre mat was bound with PCL prior to moulding, the high temperature and pressure during LS and ISP composites manufacture could have induces a level of off-axis fibre filaments, which could have potentially become unidirectionally reoriented during the fatigue cyclic loading, consequently leading to the initial increase in stiffness observed. Similar behaviour was observed in natural fibre reinforced polyester composites, in which the fibrils of the plant fibre reoriented during tensile fatigue tests and initially increased the composite stiffness [44, 63]. In addition, Betanzos et. al [15] applied cyclic pressure during the compression moulding stage of PGF reinforced polylactic acid (PLA) composites, where the composites showed significantly lower void levels, stronger matrix/fibre interfacial bonding, more uniform fibre alignment and an increase in flexural modulus. It must be noted that the initial stiffness increase was not expected and is rarely observed, further investigations into this cause will be required.

However, Figure 8b showed that the stiffness increase diminished in wet conditions, replaced by a significant decrease in stiffness from the beginning of the fatigue tests. The same change in stiffness variation was also observed when composites were tested at higher stress levels (> 50% UFS) in dry conditions. Both variations can be explained by the earlier onset and faster progress of fatigue damage caused by media attack and increased testing stresses. With the fibre/matrix de-bonding and/or fibre fractures occurring inside the composites, the effects of voids and void channels closing and/or fibre filament reorientation were insignificant. Moreover, fibre/matrix interface failure occurs readily near the void sites, which could considerably reduce the chances of voids closing due to cyclic loading [64, 65].

The wet environment also had a clear effect on the PCL/PGF composites' fatigue failure modes. Figure 11 showed that the dominant failure mode in the dry condition was compressive delamination and interlaminar shear fracture for the LS composites, whilst ISP composites showed a clean centre fracture. Immersion in PBS at 37 °C led to a distinctly more ductile behaviour (composite softening) for ISP and LS composites, which resulted from significant weakening of the fibre matrix interfaces. Figure 11f even showed the fibres sliding out sideways as the loading cycles continued, indicating loss of the fibre/matrix interface had occurred. Comparing Figures 7a and 7b, the overall strain to failure was significantly increased ($p<0.01$) by the introduction of PBS for both ISP and LS composites, which correlated well with the change from brittle to more ductile dominated failure mode. This suggested that considerably more plastic deformation and fatigue damage had

occurred in wet conditions. The immersion in PBS solution also led to lower critical applied load (See Table 5), which indicated that earlier onset of progressive fatigue damage had occurred for the wet composites.

4.3. Influence of fibre content

It is well known that the mechanical properties of fibre reinforced composites can be adjusted by varying their fibre volume fraction (V_f). The behaviour of fibre reinforced composites under cyclic loading is also significantly affected by fibre content [66, 67]. In dry conditions, the quasi-static data in Table 3 showed that the UFS increased with increasing V_f for both LS and ISP composites. Meanwhile, in wet conditions, the UFS decreased with increasing V_f for both LS and ISP composites. As mentioned earlier, the reduction in UFS was mainly caused by plasticisation due to PBS ingress along the fibres disrupting the fibre matrix interface, which severely reduced interfacial strength, and hence the reduction in UFS was seen. With increasing fibre content, there was much greater fibre/matrix interfacial area, hence the reduction of UFS was found to be more substantial in the higher volume fraction composites.

Regardless of the testing conditions, it can be seen from Figures 6a and 6b that the composites' fatigue life decreased significantly ($p<0.01$) with increasing fibre content for both LS and ISP composites. Many studies have reported that composite fatigue resistance had a tendency to deteriorate with increasing fibre volume fraction [68-70]. There are three main reasons responsible for this reduction: (i) increased fibre-fibre interactions, (ii) increased fibre/matrix interfaces and (iii) increased regions with high local V_f resulting from increased fibre bundle compaction. Although it is widely recognized that enhancement of composite mechanical properties result from effective stress transfer through fibre/matrix interfaces, it must also be noted that the fibre/matrix interface is also the region subject to the largest stress/strain variation [31]. Thus, micro-cracks mostly tend to initiate and grow from the interfaces [31]. Comparing Figures 10a and 10c to 10b and 10d, it was evident that PGFs were significantly more compacted with much more fibres close to or touching each other in the 50% V_f composites than in the 35% V_f composites. This resulted in higher stress/strain gradients at the interface and hence accelerated crack propagation, reducing fatigue life.

In dry conditions, both LS and ISP composites demonstrated a higher critical loading value for damage initiation with increasing fibre content (See Table 5). However, in wet conditions,

a lower critical loading value was noted with increasing fibre content for both of the LS and ISP composites (See Table 5). This suggested that increasing fibre content could lead to lower stress thresholds for onset of composite fatigue failure in wet conditions. On the other hand, no significant difference ($p>0.05$) was found in the degradation rate of composites fatigue strength (b coefficient) between 35% and 50% V_f composites when the same manufacturing technique was applied (see Table 4). This indicated that the degradation rate of fatigue strength could be independent on fibre content for PCL/PGF LS and ISP composites. This behaviour also suggested that increasing fibre content didn't have a significant effect on the rate of fatigue damage accumulation. Similar behaviour of composites was also described by Shah et al. [71] where no significant variation in degradation rate of fatigue strength was noted due to varying fibre content for natural fibre composites.

This paper reports for the first time the cyclic fatigue behaviour of fully bioresorbable PCL/PGF composites. Studies demonstrated that ISP composites had a significantly longer flexural fatigue life ($p<0.0001$) and superior fatigue damage resistance in comparison to their LS counterparts. The presence of media (PBS in this case) substantially reduced the performance of the PCL/PGF composites in both fatigue life and damage resistance. Increasing fibre content (from 35% to 50%) also resulted in reduced fatigue life, but no significant difference was observed for the degradation of composite fatigue strength and damage accumulation behaviours. Amongst all the composites investigated, the ISP35 samples showed a minimum fatigue life of 10^5 and 10^6 cycles up to 50% test stress levels in dry and wet conditions respectively (See Figure 6). The ISP35 also maintained at least 50% of its initial stiffness and strength (~6.5 GPa; ~ 85 MPa) at the end of the fatigue tests in both dry and wet conditions (See Figure 8), which was comparable to the flexural properties of human cortical bone (5 – 23 GPa; 35-280 MPa) [53]. Therefore, it can be advised that the fatigue life and the degradation profile of fatigue strength observed for ISP35 composites were well matched with human cortical bones, suggesting their potential suitability for bone fracture fixation applications.

5. Conclusions

Wet and dry fatigue behaviour of PCL/PGF composites (ISP and LS) was investigated in this paper. Significantly longer flexural fatigue life ($p<0.0001$) and superior fatigue damage resistance were observed for ISP composites than LS composites in both dry and wet

conditions, which indicated that the ISP process promoted considerably stronger interfacial bonding than the LS processes. Immersion in PBS during the flexural fatigue tests resulted in significant reduction ($p<0.0001$) of the composites fatigue life, earlier onset of fatigue damage and faster damage propagation. This was attributed to interface plasticisation (fibre/matrix) caused by PBS diffusion, which resulted in severely weakened interfacial strength, thus adversely affecting both the quasi-static and fatigue performances of the PCL/PGF composites. Regardless of testing conditions, increasing fibre content (from 35% to 50%) resulted in shorter fatigue life for the PCL/PGF composites. However, the degradation rate of fatigue strength and damage accumulation rate were not significantly affected by increasing fibre content. Interlaminar shear fracture and clean centre fracture were observed as the dominant failure modes for LS and ISP composites respectively in the dry condition. Meanwhile, media immersion resulted in both LS and ISP composites being softened during the fatigue tests, which led to a more ductile failure mode.

In conclusion, this paper demonstrated for the first time the flexural cyclic fatigue behaviour of fully bioresorbable ISP and LS PCL/PGF composites. ISP35 maintained at least 50% of its flexural strength and modulus after the fatigue tests, which was well within the range of the mechanical properties of the human cortical bones.

Acknowledgements

The author would like to acknowledge the University of Nottingham for awarding this studentship through the Dean of Engineering Research Scholarship for International Excellence. This research did not receive any specific grant from funding agencies in the public, commercial, or not-for-profit sectors.

References

[1] Langer R. Tissue Engineering: A New Field and Its Challenges. Pharm Res 1997;14:840-1.
[2] Hubbell JA. Biomaterials in Tissue engineering. Nature Publishing Company 1995;13:565-76.
[3] Ahmed I, Cronin PS, Abou Neel EA, Parsons AJ, Knowles JC, Rudd CD. Retention of mechanical properties and cytocompatibility of a phosphate-based glass fiber/polylactic acid composite. Journal of Biomedical Materials Research Part B: Applied Biomaterials 2009;89B:18-27.
[4] Ahmed I, Parsons AJ, Palmer G, Knowles JC, Walker GS, Rudd CD. Weight loss, ion release and initial mechanical properties of a binary calcium phosphate glass fibre/PCL composite. Acta biomaterialia 2008;4:1307-14.

[5] Felfel RM, Ahmed I, Parsons AJ, Walker GS, Rudd CD. In vitro degradation, flexural, compressive and shear properties of fully bioresorbable composite rods. Journal of the Mechanical Behavior of Biomedical Materials 2011;4:1462-72.
[6] Parsons A, Ahmed I, Niazi M, Habeb R, Fitzpatrick B, Walker G, et al. Mechanical and degradation properties of phosphate based glass fibre/PLA composites with different fibre treatment regimes. Science and Engineering of Composite Materials 2010;17:243-60.
[7] Brauer D, Rüssel C, Vogt S, Weisser J, Schnabelrauch M. Degradable phosphate glass fiber reinforced polymer matrices: mechanical properties and cell response. J Mater Sci: Mater Med 2008;19:121-7.
[8] Knowles JC. Phosphate based glasses for biomedical applications. Journal of Materials Chemistry 2003;13:2395-401.
[9] Lehtonen TJ, Tuominen JU, Hiekkanen E. Dissolution behavior of high strength bioresorbable glass fibers manufactured by continuous fiber drawing. Journal of the Mechanical Behavior of Biomedical Materials 2013;20:376-86.
[10] Parsons AJ, Ahmed I, Haque P, Fitzpatrick B, Niazi MIK, Walker GS, et al. Phosphate Glass Fibre Composites for Bone Repair. Journal of Bionic Engineering 2009;6:318-23.
[11] Mohammadi MS, Ahmed I, Muja N, Rudd CD, Bureau MN, Nazhat SN. Effect of phosphate-based glass fibre surface properties on thermally produced poly(lactic acid) matrix composites. Journal of materials science Materials in medicine 2011;22:2659-72.
[12] Ahmed I, Collins CA, Lewis MP, Olsen I, Knowles JC. Processing, characterisation and biocompatibility of iron-phosphate glass fibres for tissue engineering. Biomaterials 2004;25:3223-32.
[13] Chen M, Parsons AJ, Felfel RM, Rudd CD, Irvine DJ, Ahmed I. In-situ polymerisation of fully bioresorbable polycaprolactone/phosphate glass fibre composites: In vitro degradation and mechanical properties. Journal of the mechanical behavior of biomedical materials 2016;59:78-89.
[14] Hasan M, Ahmed I, Parsons A, Walker G, Scotchford C. Cytocompatibility and Mechanical Properties of Short Phosphate Glass Fibre Reinforced Polylactic Acid (PLA) Composites: Effect of Coupling Agent Mediated Interface. Journal of Functional Biomaterials 2012;3:706-25.
[15] Barrera Betanzos F, Gimeno-Fabra M, Segal J, Grant D, Ahmed I. Cyclic pressure on compression-moulded bioresorbable phosphate glass fibre reinforced composites. Materials & Design 2016;100:141-50.
[16] Jiang G, Evans ME, Jones IA, Rudd CD, Scotchford CA, Walker GS. Preparation of poly(ε-caprolactone)/continuous bioglass fibre composite using monomer transfer moulding for bone implant. Biomaterials 2005;26:2281-8.
[17] Corden TJ, Jones IA, Rudd CD, Christian P, Downes S. Initial development into a novel technique for manufacturing a long fibre thermoplastic bioabsorbable composite: in-situ polymerisation of poly-ϵ-caprolactone. Composites Part A: Applied Science and Manufacturing 1999;30:737-46.
[18] Christian P, Jones IA, Rudd CD, Campbell RI, Corden TJ. Monomer transfer moulding and rapid prototyping methods for fibre reinforced thermoplastics for medical applications. Composites Part A: Applied Science and Manufacturing 2001;32:969-76.
[19] Corden TJ, Jones IA, Rudd CD, Christian P, Downes S, McDougall KE. Physical and biocompatibility properties of poly-ε-caprolactone produced using in situ polymerisation: a novel manufacturing technique for long-fibre composite materials. Biomaterials 2000;21:713-24.
[20] McKibbin B. The biology of fracture healing in long bones. J Bone Joint Surg [Br: Citeseer; 1978.

[21] Giannoudis PV, Einhorn TA, Marsh D. Fracture healing: The diamond concept. Injury 2007;38:S3-S6.
[22] An YH, Woolf SK, Friedman RJ. Pre-clinical in vivo evaluation of orthopaedic bioabsorbable devices. Biomaterials 2000;21:2635-52.
[23] Frost H. The biology of fracture healing: an overview for clinicians. Part I. Clinical orthopaedics and related research 1989;248:283-93.
[24] Liao K, Schultheisz CR, Hunston DL, Brinson LC. Long-term durability of fiber-reinforced polymer-matrix composite materials for infrastructure applications: a review. Journal of advanced materials 1998;30:3-40.
[25] Vauthier E, Abry J, Bailliez T, Chateauminois A. Interactions between hygrothermal ageing and fatigue damage in unidirectional glass/epoxy composites. Composites Science and Technology 1998;58:687-92.
[26] Jones C, Dickson R, Adam T, Reiter H, Harris B. The environmental fatigue behaviour of reinforced plastics. Proceedings of the Royal Society of London A: Mathematical, Physical and Engineering Sciences: The Royal Society; 1984. p. 315-38.
[27] Malpot A, Touchard F, Bergamo S. Influence of moisture on the fatigue behaviour of a woven thermoplastic composite used for automotive application. Materials & Design 2016;98:12-9.
[28] Stinchcomb W, Reifsnider K. Fatigue damage mechanisms in composite materials: a review. Fatigue mechanisms: ASTM International; 1979.
[29] Sakin R, Ay İ, Yaman R. An investigation of bending fatigue behavior for glass-fiber reinforced polyester composite materials. Materials & Design 2008;29:212-7.
[30] Liang S, Gning PB, Guillaumat L. A comparative study of fatigue behaviour of flax/epoxy and glass/epoxy composites. Composites Science and Technology 2012;72:535-43.
[31] Vassilopoulos AP, Keller T. Fatigue of fiber-reinforced composites: Springer Science & Business Media; 2011.
[32] Caprino G, D'Amore A. Flexural fatigue behaviour of random continuous-fibre-reinforced thermoplastic composites. Composites Science and Technology 1998;58:957-65.
[33] Cox BN, Marshall DB. CRACK BRIDGING IN THE FATIGUE OF FIBROUS COMPOSITES. Fatigue & Fracture of Engineering Materials & Structures 1991;14:847-61.
[34] Hamad WY. On the mechanisms of cumulative damage and fracture in native cellulose fibres. Journal of Materials Science Letters 1998;17:433-6.
[35] Aghazadeh Mohandesi J, Majidi B. Fatigue damage accumulation in carbon/epoxy laminated composites. Materials & Design 2009;30:1950-6.
[36] Shiri S, Yazdani M, Pourgol-Mohammad M. A fatigue damage accumulation model based on stiffness degradation of composite materials. Materials & Design 2015;88:1290-5.
[37] Hwang SJ, Gibson RF, Singh J. Decomposition of coupling effects on damping of laminated composites under flexural vibration. Composites Science and Technology 1992;43:159-69.
[38] Gassan J. A study of fibre and interface parameters affecting the fatigue behaviour of natural fibre composites. Composites Part A: Applied Science and Manufacturing 2002;33:369-74.
[39] Lu J, Sun W, Becker A, Saad AA. Simulation of the fatigue behaviour of a power plant steel with a damage variable. International Journal of Mechanical Sciences 2015;100:145-57.
[40] Mao H, Mahadevan S. Fatigue damage modelling of composite materials. Composite Structures 2002;58:405-10.
[41] Wu F, Yao W. A fatigue damage model of composite materials. International Journal of Fatigue 2010;32:134-8.

[42] Gamstedt EK, Berglund LA, Peijs T. Fatigue mechanisms in unidirectional glass-fibre-reinforced polypropylene. Composites Science and Technology 1999;59:759-68.
[43] Lu J, Sun W, Becker A. Material characterisation and finite element modelling of cyclic plasticity behaviour for 304 stainless steel using a crystal plasticity model. International Journal of Mechanical Sciences 2016;105:315-29.
[44] Shah DU. Damage in biocomposites: Stiffness evolution of aligned plant fibre composites during monotonic and cyclic fatigue loading. Composites Part A: Applied Science and Manufacturing 2016;83:160-8.
[45] The Mechanical Properties of Cortical Bone1974.
[46] Bian D, Zhou W, Liu Y, Li N, Zheng Y, Sun Z. Fatigue behaviors of HP-Mg, Mg–Ca and Mg–Zn–Ca biodegradable metals in air and simulated body fluid. Acta biomaterialia 2016;41:351-60.
[47] van den Oever M, Peijs T. Continuous-glass-fibre-reinforced polypropylene composites II. Influence of maleic-anhydride modified polypropylene on fatigue behaviour. Composites Part A: Applied Science and Manufacturing 1998;29:227-39.
[48] Reifsnider KL, Schulte K, Duke JC. Long-term fatigue behavior of composite materials. Long-term behavior of composites: ASTM International; 1983.
[49] Adams RD, Bacon DGC. Measurement of the flexural damping capacity and dynamic Young's modulus of metals and reinforced plastics. Journal of Physics D: Applied Physics 1973;6:27.
[50] Felfel R, Hossain KZ, Parsons A, Rudd C, Ahmed I. Accelerated in vitro degradation properties of polylactic acid/phosphate glass fibre composites. Journal of Materials Science 2015;50:3942-55.
[51] Ramakrishnan V, Jayaraman N. Mechanistically based fatigue-damage evolution model for brittle matrix fibre-reinforced composites. Journal of Materials Science 1993;28:5592-602.
[52] Keusch S, Queck H, Gliesche K. Influence of glass fibre/epoxy resin interface on static mechanical properties of unidirectional composites and on fatigue performance of cross ply composites. Composites Part A: Applied Science and Manufacturing 1998;29:701-5.
[53] Bao G, Song Y. Crack bridging models for fiber composites with slip-dependent interfaces. Journal of the Mechanics and Physics of Solids 1993;41:1425-44.
[54] Subramanian S, Elmore JS, Stinchcomb WW, Reifsnider KL. Influence of fiber-matrix interphase on the long-term behavior of graphite/epoxy composites. Composite Materials: Testing and Design: Twelfth Volume: ASTM International; 1996.
[55] Shih GC, Ebert LJ. The effect of the fiber/matrix interface on the flexural fatigue performance of unidirectional fiberglass composites. Composites Science and Technology 1987;28:137-61.
[56] Bledzki A, Wacker G, Frenzel H. Effect of surface-treated glass fibres on the dynamic behavior of fibre-reinforced composites. Mechanics of composite materials 1994;29:429-33.
[57] Kotsikos G, Evans JT, Gibson AG, Hale JM. Environmentally enhanced fatigue damage in glass fibre reinforced composites characterised by acoustic emission. Composites Part A: Applied Science and Manufacturing 2000;31:969-77.
[58] Houghton W, Shuford R, Mitchel J, Sobczak J. NDE of composite rotor blades during fatigue testing. Proceedings of the Helicopter Society of America Conference, St Louis1980.
[59] Liao K, Schultheisz CR, Hunston DL. Long-term environmental fatigue of pultruded glass-fiber-reinforced composites under flexural loading. International journal of fatigue 1999;21:485-95.

[60] McBagonluri F, Garcia K, Hayes M, Verghese K, Lesko J. Characterization of fatigue and combined environment on durability performance of glass/vinyl ester composite for infrastructure applications. International journal of fatigue 2000;22:53-64.
[61] Shan Y, Liao K. Environmental fatigue behavior and life prediction of unidirectional glass–carbon/epoxy hybrid composites. International Journal of Fatigue 2002;24:847-59.
[62] Sumsion H, Williams D. Effects of environment on the fatigue of graphite-epoxy composites. Fatigue of composite materials: ASTM International; 1975.
[63] Shah DU. Developing plant fibre composites for structural applications by optimising composite parameters: a critical review. Journal of Materials Science 2013;48:6083-107.
[64] Chambers AR, Earl JS, Squires CA, Suhot MA. The effect of voids on the flexural fatigue performance of unidirectional carbon fibre composites developed for wind turbine applications. International Journal of Fatigue 2006;28:1389-98.
[65] Thomason JL. The interface region in glass fibre-reinforced epoxy resin composites: 2. Water absorption, voids and the interface. Composites 1995;26:477-85.
[66] Chandra R, Singh S, Gupta K. Damping studies in fiber-reinforced composites–a review. Composite structures 1999;46:41-51.
[67] Saravanos DA, Chamis CC. Unified micromechanics of damping for unidirectional and off-axis fiber composites. Journal of Composites, Technology and Research 1990;12:31-40.
[68] Mandell JF, Reed RM, Samborsky DD. Fatigue of fiberglass wind turbine blade materials.
[69] Samborsky DD. Fatigue of E-glass fiber reinforced composite materials and substructures: Citeseer; 1999.
[70] Boller KH. Effect of tensile mean stresses on fatigue properties of plastic laminates reinforced with unwoven glass fibers. DTIC Document; 1964.
[71] Shah DU, Schubel PJ, Clifford MJ, Licence P. Fatigue life evaluation of aligned plant fibre composites through S–N curves and constant-life diagrams. Composites Science and Technology 2013;74:139-49.

Table 1: Phosphate glass code and formulation

Glass code	P_2O_5 content (mol%)	CaO content (mol%)	Na_2O content (mol%)	MgO content (mol%)	Fe_2O_3 content (mol%)	Drying temp/time (°C/h)	Melting temp/time (°C/h)
P45Fe5	45	16	10	24	5	350/0.5	1100/1.5

Table 2: PCL/PGF composites codes (D/W refers to dry or wet testing conditions)

Manufacture technique	Composites codes	Fibre Orientation
Laminate Stacking (LS)	(D/W)-LS35	Unidirectional (UD)
	(D/W)-LS50	
In-situ Polymerisation (ISP)	(D/W)-ISP35	
	(D/W)-ISP50	

Table 3. Quasi-static flexural properties for all composite specimens

Composites Code	**Actual V_f (%)**	**Ultimate Flexural Strength (UFS) (MPa)**	**Flexural Stiffness (E_f) (GPa)**	**Composites Code**	**Actual V_f (%)**	**Ultimate Flexural Strength (UFS) (MPa)**	**Flexural Stiffness (E_f) (GPa)**
D-LS35	34 ± 1	126 ± 2	9.1 ± 0.7	**D-ISP35**	36 ± 1	172 ± 3	14.4 ± 0.6
W-LS35	32 ± 1	110 ± 3	6.2 ± 0.3	**W-ISP35**	35 ± 1	141 ± 2	13.0 ± 0.2
D-LS50	51 ± 1	143 ± 2	12.7 ± 0.4	**D-ISP50**	49 ± 2	210 ± 3	18.6 ± 0.4
W-LS50	50 ± 1	105 ± 1	6.3 ± 0.3	**W-ISP50**	50 ± 1	123 ± 1	12.4 ± 0.4

Table 4. Values of *'b'* from S-N curve fitting for LS and ISP composites

Sample Code	**D-LS35**	**D-LS50**	**W-LS35**	**W-LS50**	**D-ISP35**	**D-ISP50**	**W-ISP35**	**W-ISP50**
b	-0.089	-0.071	-0.497	-0.661	-0.101	-0.131	-0.241	-0.244

Table 5. Values of Critical Applied Stress (CAS) for LS and ISP composites

Sample Code	**D-LS35**	**D-LS50**	**D-ISP35**	**D-ISP50**	**W-LS35**	**W-LS50**	**W-ISP35**	**W-ISP50**
CAS (MPa)	63	71	103	126	44	42	56	49

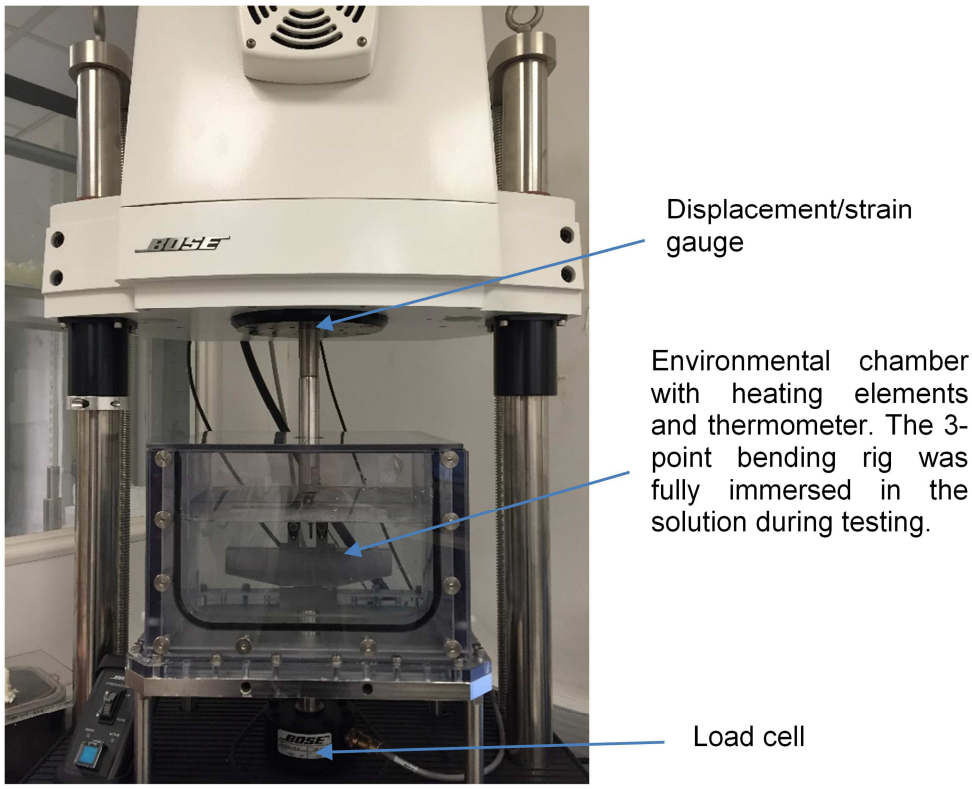

Figure 1. Bose ElectroForce® Series II 3330 testing machine equipped with environmental chamber

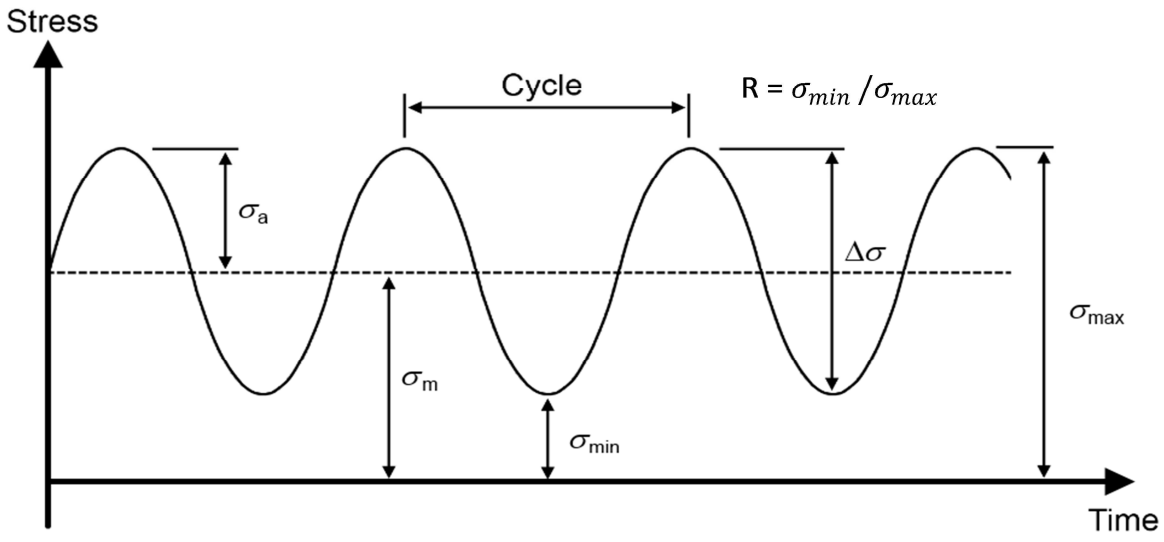

Figure 2. Example of sinusoidal constant amplitude load waveforms with term definition and R value

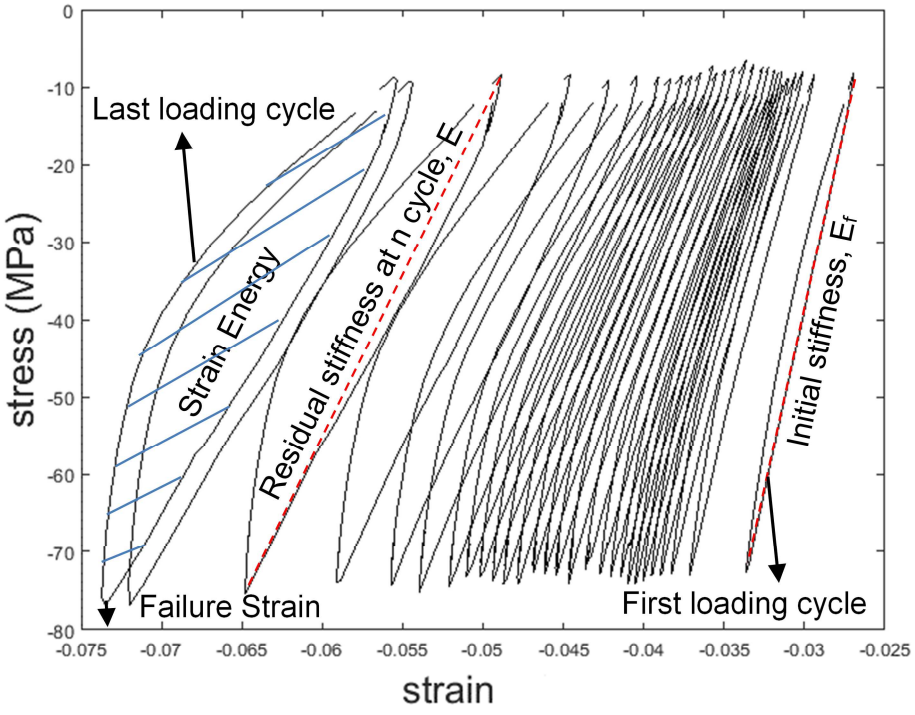

Figure 3. Example of stress strain variation during the flexural fatigue tests (the negative sign only indicated the direction as downwards)

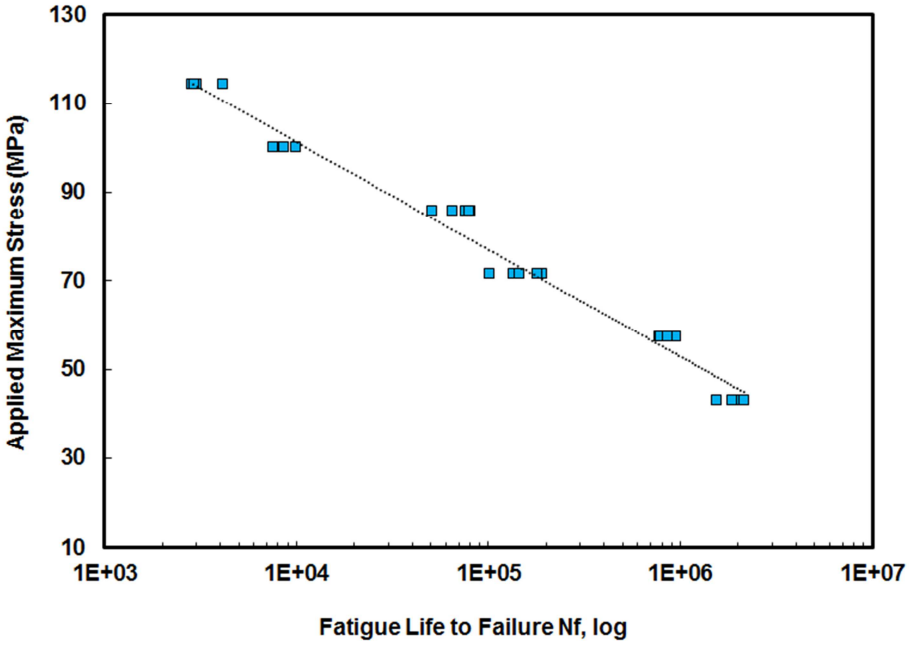

Figure 4. Typical S-N diagram with example data

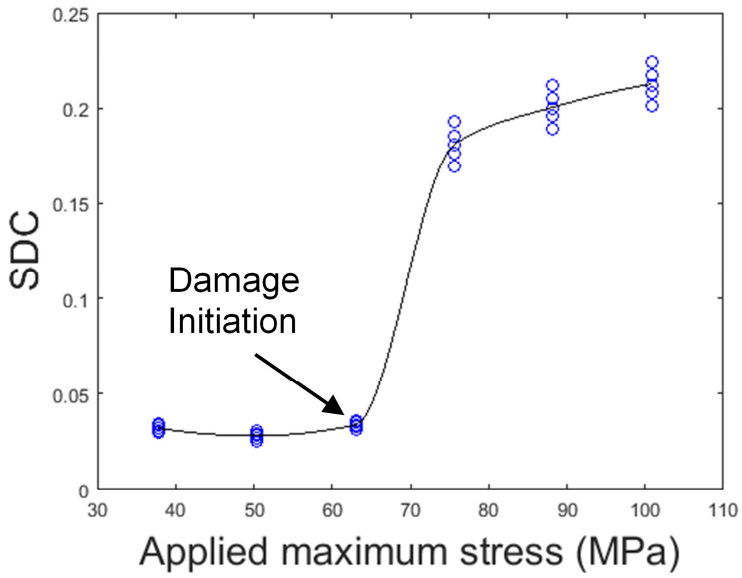

Figure 5. Example of Specific Flexural Damping Capacity vs. Applied Maximum Stress for dry LS35 composites

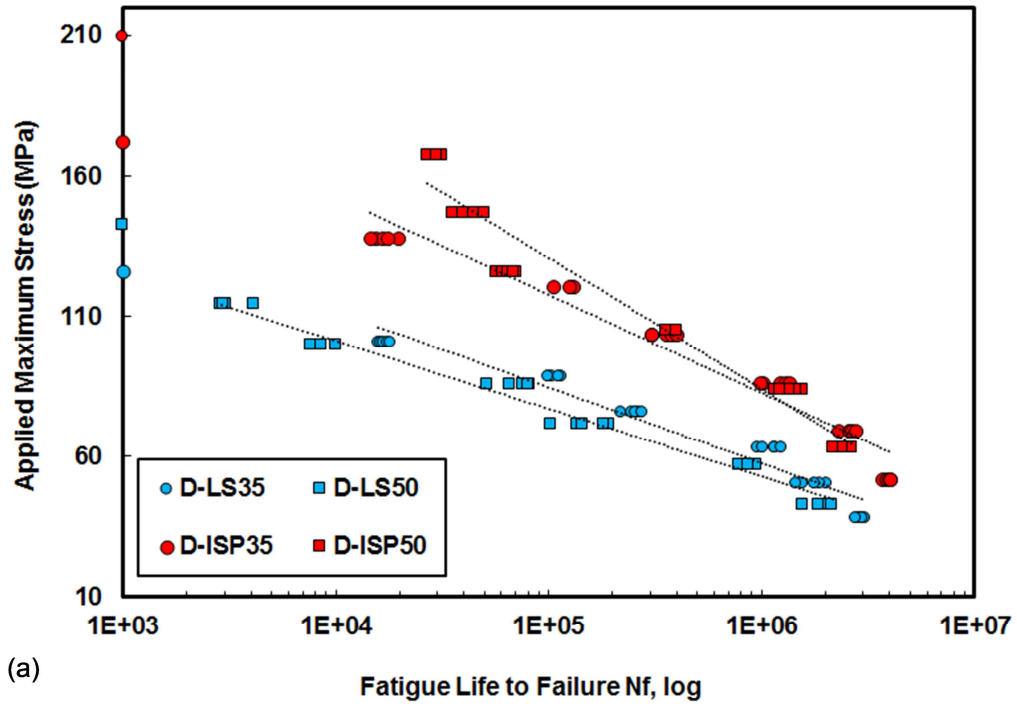

(a)

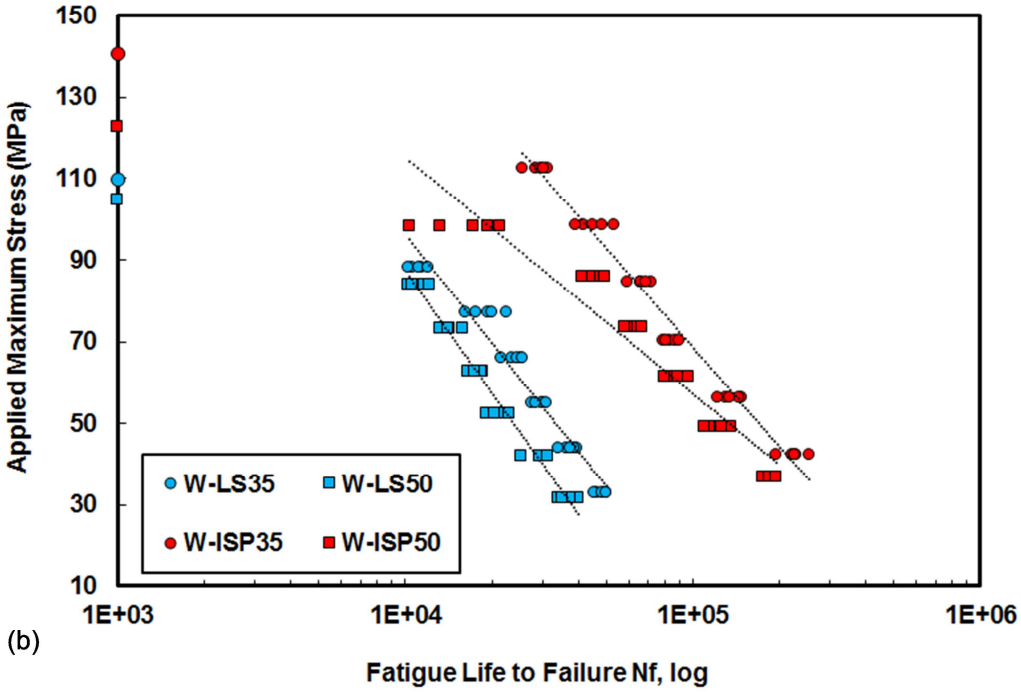

(b)

Figure 6. S-N diagram of PCL/PGF composites in dry and wet environments plotted in power-law regression scale (points on the y-axis indicate the monotonic flexural strength of the composites): (a) Comparison of composites made by LS and ISP in dry environment; (b) Comparison of composites made by LS and ISP in wet environment. The circles represent 35% V_f whereas the squared points are representative of 50% V_f samples.

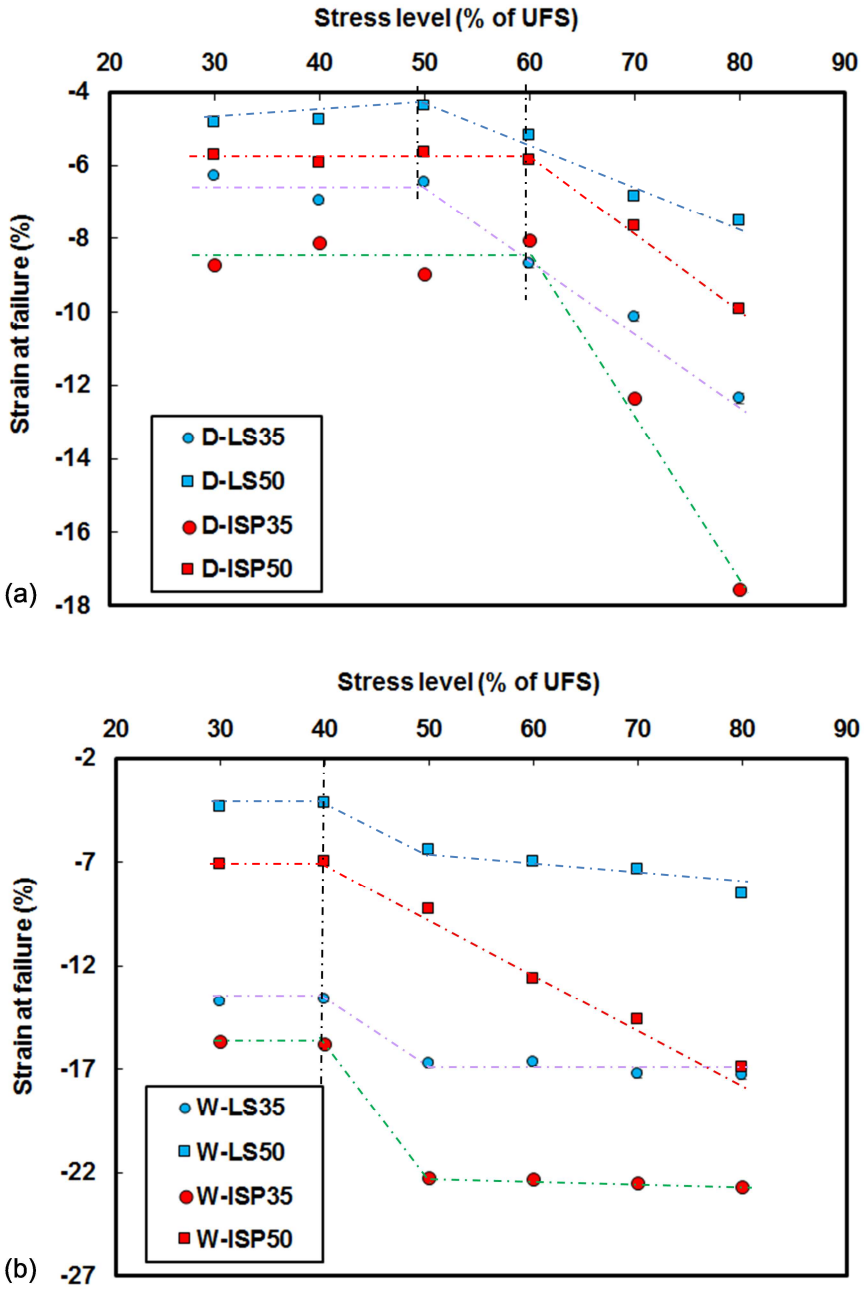

Figure 7. Strain at fatigue failure ('-' as downwards) against testing stress levels: (a) LS and ISP composites tested dry; (b) LS and ISP composites tested wet; Error bars fall within the dimension of the markers. Vertical dotted line presents threshold stress level that the failure strains increase significantly, other dotted lines are given as guides to the eyes

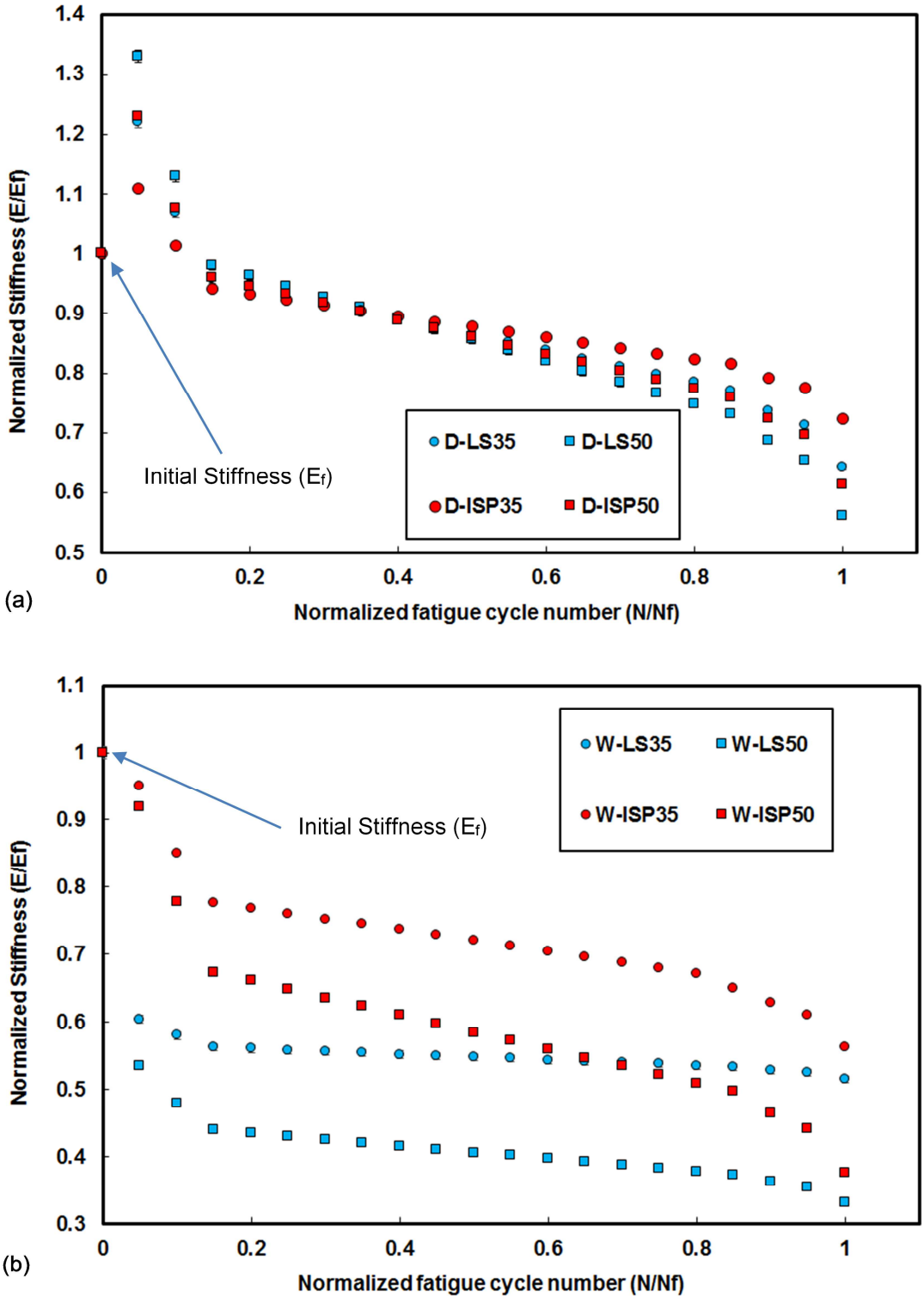

Figure 8. Normalised stiffness against normalised cycle number for composites tested at 40% of UFS in: (a) Dry Environment, inset graph for dry composites tested at 60% of UFS; (b) Wet Environment; Error bars fall within the dimension of the markers

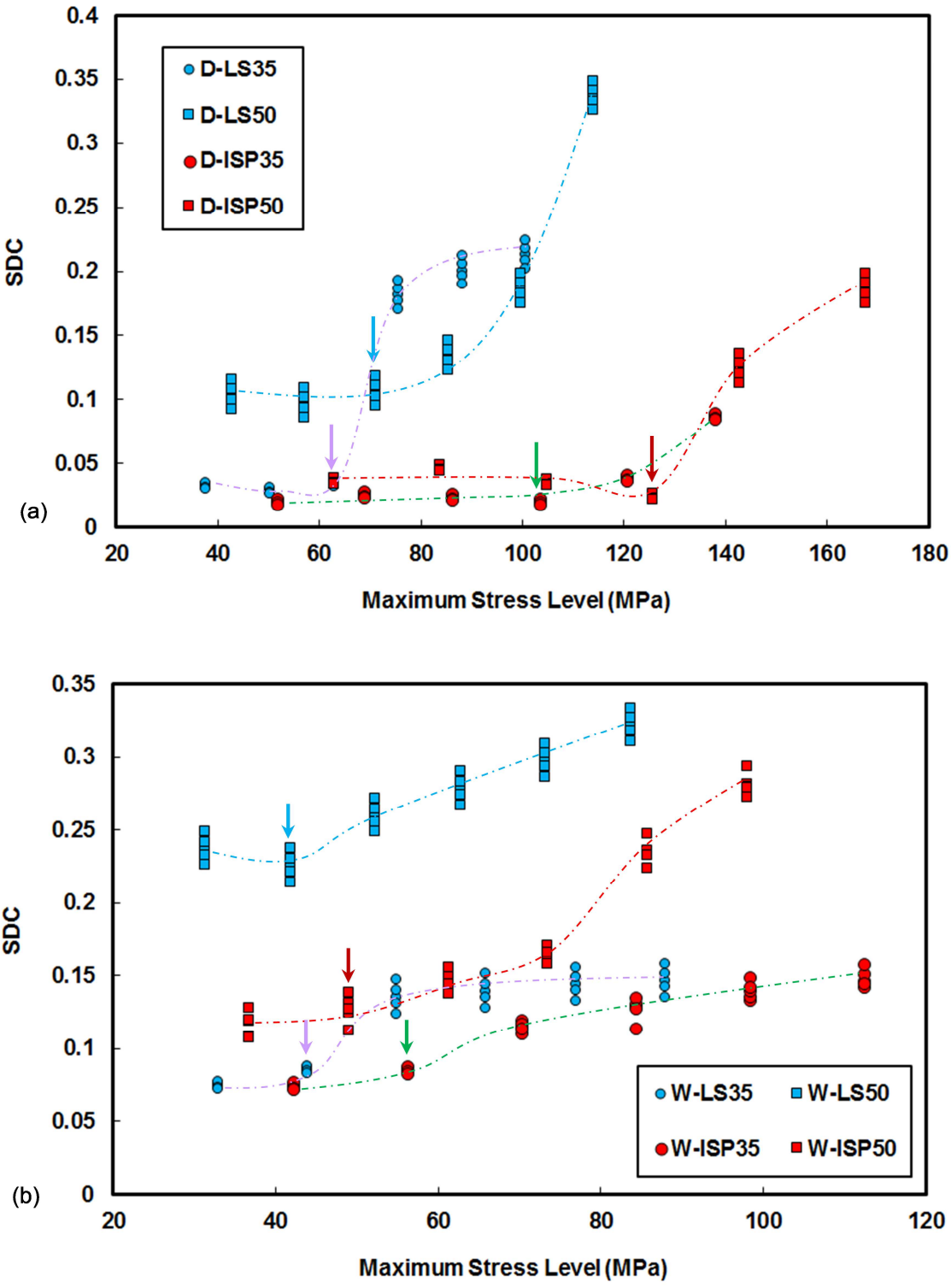

Figure 9. Specific flexural damping capacity verses applied maximum load for LS and ISP composites: (a) in dry conditions; (b) in wet conditions; Arrows point to the CAS values of the composites. The dotted lines are given as guides to the eye

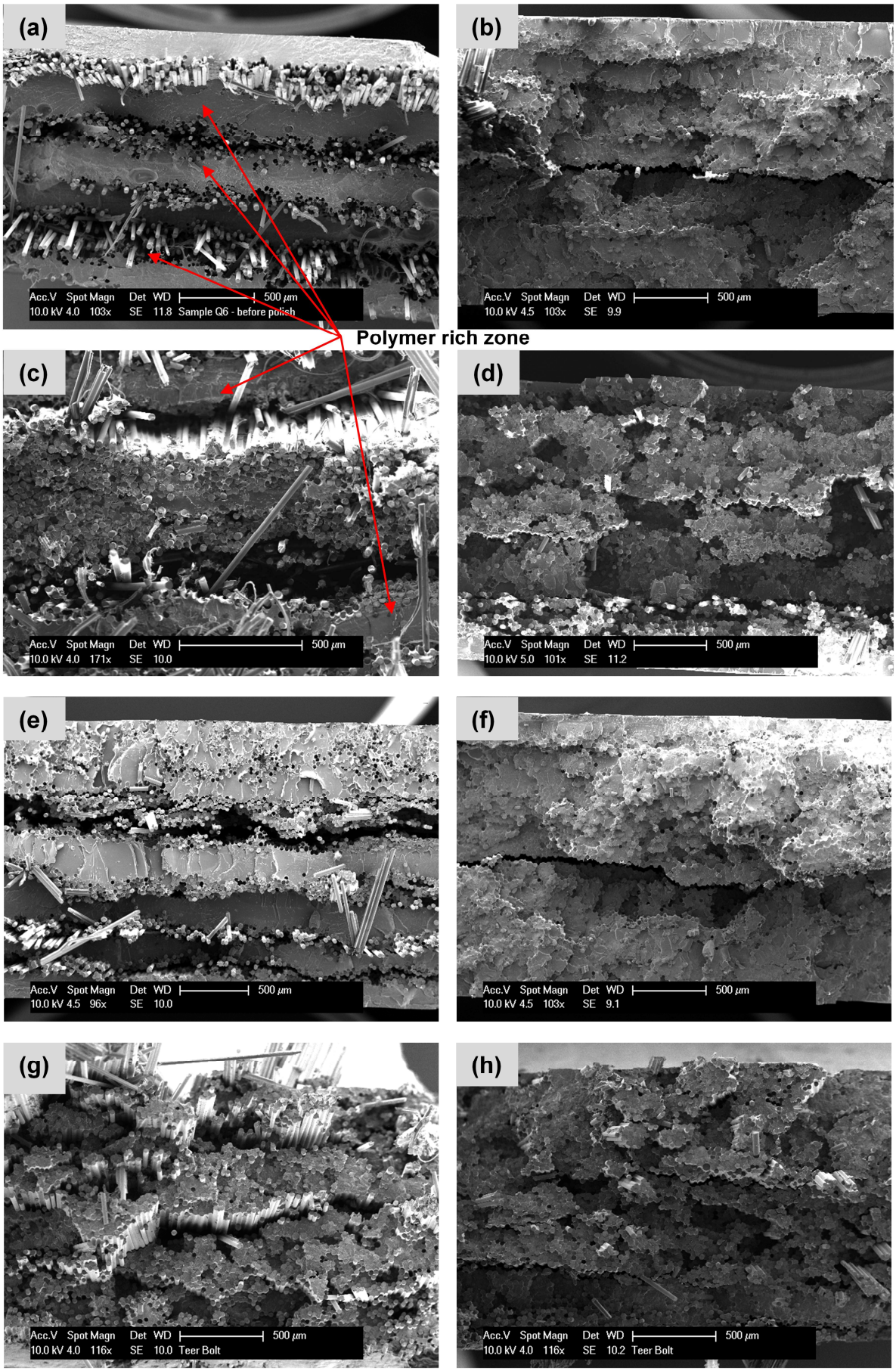
(a)
Acc.V Spot Magn Det WD 500 µm
10.0 kV 4.0 103x SE 11.8 Sample Q6 - before polish
(b)
Acc.V Spot Magn Det WD 500 µm
10.0 kV 4.5 103x SE 9.9
Polymer rich zone
(c)
Acc.V Spot Magn Det WD 500 µm
10.0 kV 4.0 171x SE 10.0
(d)
Acc.V Spot Magn Det WD 500 µm
10.0 kV 5.0 101x SE 11.2
(e)
Acc.V Spot Magn Det WD 500 µm
10.0 kV 4.5 96x SE 10.0
(f)
Acc.V Spot Magn Det WD 500 µm
10.0 kV 4.5 103x SE 9.1
(g)
Acc.V Spot Magn Det WD 500 µm
10.0 kV 4.0 116x SE 10.0 Teer Bolt
(h)
Acc.V Spot Magn Det WD 500 µm
10.0 kV 4.0 116x SE 10.2 Teer Bolt

Figure 10. SEM cross section images of the composites fatigue fracture surfaces: (a) D -LS35; (b) D -ISP35; (c) D -LS50; (d) D -ISP50; (e) W -LS35; (f) W -ISP35; (g) W -LS50; (h) W -ISP50

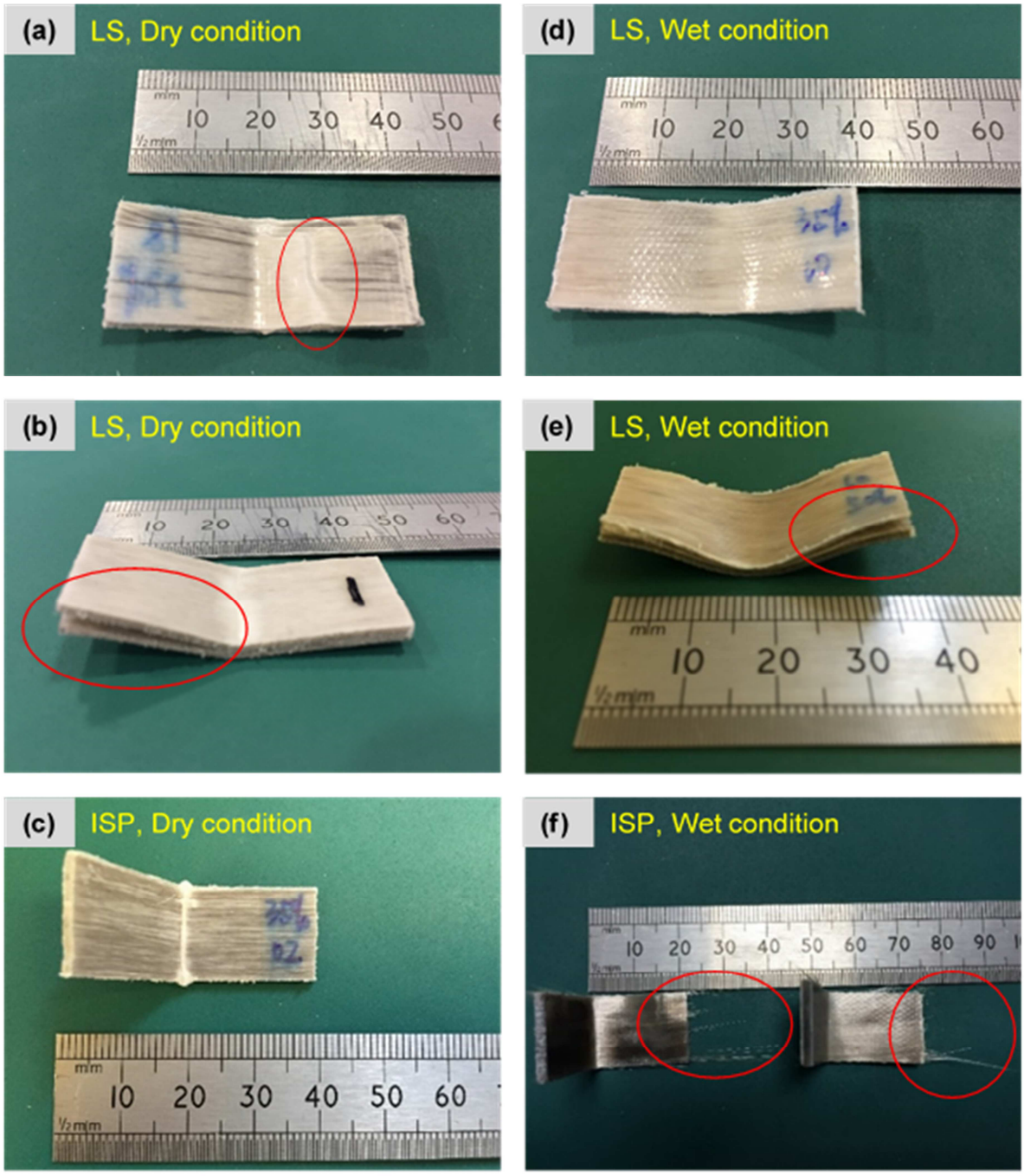

Figure 11. Images taken of LS and ISP composites' after end of fatigue testing cycles: (a) compressive delamination was observed (see red circle); (b) interlaminar shear fracture (see red circle); (c) centre fracture where load was applied; (d) softening of sample observed from wet testing; (e) softening and interlaminar shear fracture observed (see red circle); (f) fibre protrusions were also observed post testing (see red circles) and centre fracture were load was applied.